Miscibility of Gramicidin A−Ethyl Nonadecanoate in Langmuir Monolayers in the Presence of Salts Dissolved in the Subphase

N. Vila-Romeu,*,† M. Nieto-Suárez,† and P. Dynarowicz-Łątka‡

Department of Physical Chemistry−Faculty of Sciences, University of Vigo, Campus As Lagoas s/n 32004 Ourense, Spain, and Faculty of Chemistry, Jagiellonian University, Kraków, Poland

Received: February 22, 2005; In Final Form: June 14, 2005

The behavior of binary mixed Langmuir monolayers from gramicidin A (GA) and ethyl nonadecanoate (EN), spread on aqueous subphases containing NaCl and $CaCl_2$, was investigated on the basis of the analysis of surface pressure−average area per molecule ($\pi-A$) isotherms complemented with Brewster angle microscopy (BAM) images. Compression modulus versus surface pressure ($C_S^{-1}-\pi$) curves indicate the existence of interactions in the GA−EN mixed monolayers at low surface pressures (below 5 mN m^{-1}). However, for mixtures in which the ester is the predominant component, both GA and EN are miscible within regions from fully expanded to collapse. To examine the interactions between both components in the studied system, values of the mean molecular area per molecule (A_{12}) were plotted as a function of molar fraction of gramicidin A (X_{GA}). $A_{12}-X_{GA}$ plots exhibit negative deviations from ideality at high surface pressures, wherein β-helices of GA are vertically oriented in respect to the interface. However, at surface pressures below the plateau transition, which is due to reorientation of GA, the binary system obeys the additive rule. Brewster angle microscopy (BAM) was applied for a direct visualization of the monolayers morphologies. The obtained images prove that for molar ratios of GA $\geq$ 0.3 and at surface pressures above 5 mN m^{-1}, both components are immiscible at the interface. The observed negative deviations from the additively rule were attributed to the formation of a three-dimensional phase in the mixed film, which provokes its contraction at the interface.

Introduction

The antibiotic, gramicidin A, is one of the best-characterized channel-forming peptides.[1,2] It can exist in several tubular dimeric forms, two main structural types consisting of a head-to-head helical dimer and a double helical channel,[3−6] both capable of monovalent cation transport through lipid bilayers. Recent research findings suggest that upon modifying the environmental conditions, for example, the addition of ions, the solvent used, or the length of the alkyl chains of the bilayer in which the peptide is embedded, the equilibrium between these ion-conducting conformations can be shifted from one to other.[7−23]

Our investigations are aimed at designing a mimetic membrane for selective ion transport. For this purpose, peptide and lipid molecules (that serve as a model membrane) have to be miscible, and the conformation of the channel maker cannot be altered by either the presence of the model amphiphile or moderate changes in temperature.

It is well known that Langmuir monolayers[24] are appropriate models for studying the behavior and the influence of factors that can alter the functional properties of GA in two-dimensional (2D) state.[19] In the present study, ester molecules (ethyl nonadecanoate) were used as lipid matrix. They are capable of stable monolayer formation, which can subsequently be easily transferred onto solid supports.[25,26] Furthermore, esters have the advantage, over other lipids that are frequently used in many in vitro studies, of being appropriate for simulating a membrane lipid environment, because their headgroups are not charged and, therefore, reduce the likelihood of undesirable interactions with either GA or ions to be transported. With this in mind, we have investigated the behavior of mixed Langmuir monolayers of GA and EN, and we compared their $\pi-A$ isotherms with those of pure components. The experiments were performed on aqueous subphases containing NaCl or $CaCl_2$. This allowed us to analyze the influence of the presence of mono- and divalent cations on the miscibility of both molecules at the interface, as well as on the nature of interactions established between them.

Moreover, to obtain a deeper insight into the structure of such a mixed system, we have employed Brewster angle microscopy (BAM) for a direct visualization of the monolayers morphology.[27,28]

Materials and Methods

Gramicidin A (GA) (>90% pure, <H_2O 5%) was purchased from Fluka and stored at 4 °C. Ethyl palmitate (EP) (98% pure) was supplied by Sigma Chemicals, and it was stored below 0 °C. Both compounds were used as received. Spreading solutions of GA/EP were prepared by mixing appropriate volumes of stock solutions of GA and EP, both dissolved in spectroscopic grade chloroform (Merck). Langmuir monolayers were obtained by spreading an aliquot of the above-mentioned solutions. Ultrapure water, produced by a Nanopure (Infinity) water purification system coupled to a Milli-Q water purification system (resistivity = 18.2 MΩ cm), was used to prepare aqueous solutions. $CaCl_2$ (99.5%, Merck) and NaCl (99.5%, Merck) were added to ultrapure water to prepare $[Ca^{2+}] = 3 \times 10^{-3}$ M and $[Na^+] = 1 \times 10^{-2}$ M solutions onto which the monolayers were spread (the ionic strength of both solutions = 0.01 M). After spreading, the monolayers were left for 30 min, and afterward the compression was initiated. Routine monolayer studies were carried out with a NIMA 601 trough system (total area = 510 cm^2) placed on an anti-vibration table. Surface pressure was measured with the Wilhelmy plate (made of ashless filter paper) with an accuracy of ±0.1 mN m^{-1}. Monolayers were com-

* Corresponding author. Phone: +34988387095. Fax: +34988387001. E-mail: nvromeu@uvigo.es.
† University of Vigo.
‡ Jagiellonian University.

10.1021/jp050920+ CCC: $30.25
Published on Web 07/15/2005

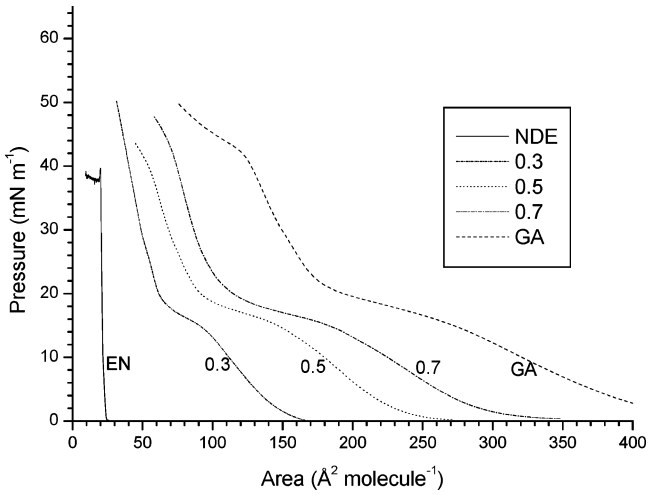

Figure 1. Surface pressure−area ($\pi-A$) isotherms of pure EN and GA monolayers and their mixtures. $T = 20$ °C. Subphase: NaCl aq, $I = 0.01$ M.

pressed with the barrier speed of 5.6 Å^2 molecule^{-1} min^{-1}. The experiments were performed at three different temperatures (15, 20, and 25 °C). The subphase temperature was controlled thermostatically to within 0.1 °C by a circulating water system.

Brewster angle microscope BAM 2 plus (NFT, Germany) was used for microscopic observation of the monolayers structure. It is equipped with a 30 mW laser, emitting p-polarized light of 690 nm wavelength, that was reflected off the air−water interface at approximately 53.1° (Brewster angle). The lateral resolution of the microscope was 2 μm. The images were digitized and processed to obtain the best quality of the BAM pictures.

Results

Surface Pressure−Area Isotherms and Compressibility of GA−EN Mixed Monolayers. Figure 1 shows the $\pi-A$ isotherms recorded upon compression of pure monolayers formed by EN and GA, and mixed films of X_{GA}: 0.3, 0.5, and 0.7 spread on NaCl subphases (ionic strength 0.01 M). The monolayers of EN are of condensed-type with the limiting area of 22 Å^2 molecule^{-1} and collapse pressure (π_c) of about 32 mN m^{-1}. The surface compression modulus [$C_S^{-1} = -A(d\pi/dA)$] versus surface pressure ($C_S^{-1}-\pi$) dependence for the investigated ester, presented in Figure 2, shows two maxima of

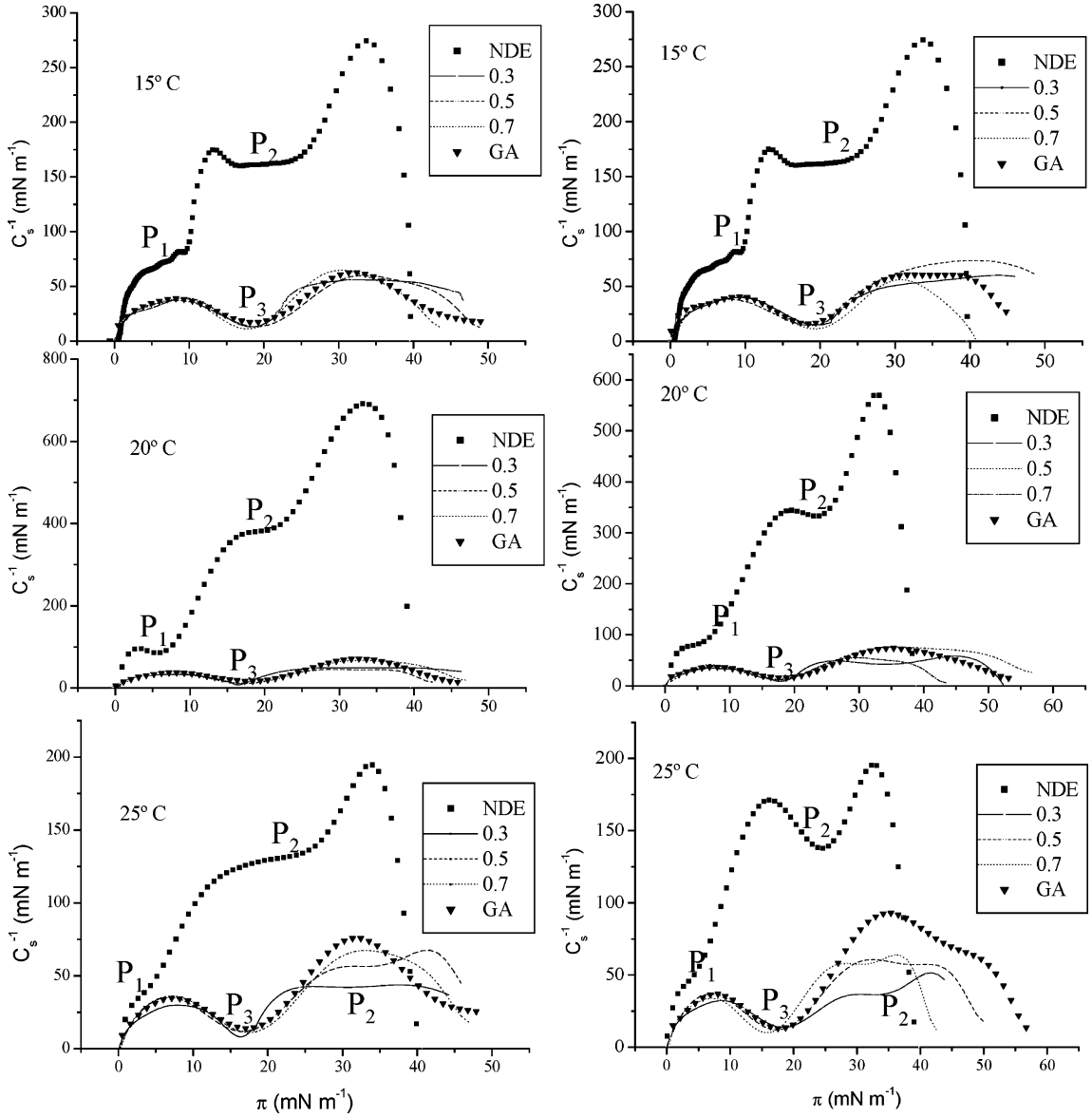

Figure 2. Plots of the compression modulus (C_S^{-1}) as a function of the surface pressure (π) at different subphase temperatures. Left column: subphase NaCl aq, $I = 0.01$ M. Right column: $CaCl_2$ aq, $I = 0.01$ M.

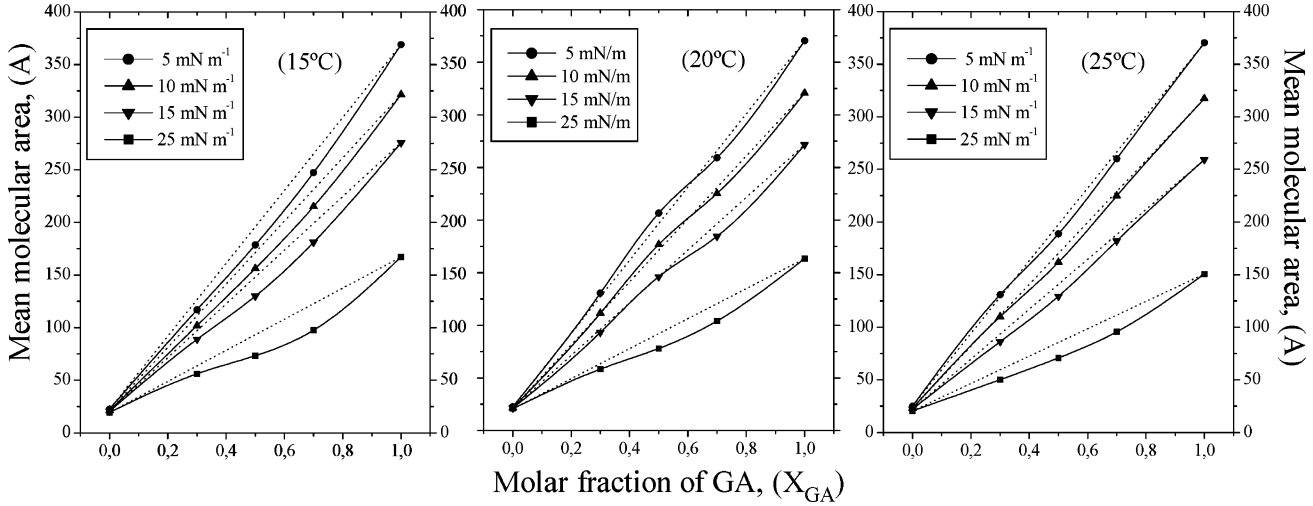

Figure 3. Plots of the mean molecular area (A_{12}) versus mole fraction of GA (X_{GA}) at different surface pressures and temperatures. Subphase: NaCl aq, $I = 0.01$ M.

high C_S^{-1} values, which are characteristic of a solid film. At surface pressures of about 5 mN m^{-1} (P_1 in Figure 2) and 20 mN m^{-1} (P_2 in Figure 2), two phase transitions, which appear as a minima in the $C_S^{-1}-\pi$ curve, can be distinguished. Interestingly, both of them are not visualized in course of the $\pi-A$ isotherm. Moderate changes in temperature (15−25 °C) do not affect values of π corresponding to phase transitions P_1 and P_2.

The isotherm of pure GA shows three distinct regions (see Figure 1): the first one, corresponding to the monolayer in its liquid expanded state; the second one, of a liquid-condensed nature, which is characterized by higher C_S^{-1} values; and the third region, which spans between the two above-mentioned regions and is represented by a plateau of a quasi constant surface pressure (π_t) at about 18 mN m^{-1}. This region is reflected in the $C_S^{-1}-\pi$ curve (see Figure 2) as a minimum P_3. This characteristic phase transition observed in the isotherm of GA has been attributed to changes in the orientation of the β-helices from a parallel to vertical position with respect to the interface prior to collapse at 30−35 mN m^{-1}.[19,29−31]

The isotherms of mixed GA/EN monolayers resemble that recorded for pure GA. All of the isotherms clearly exhibit the plateau of pure GA with a π_t value close to 18 mN m^{-1}, which practically remains constant as the temperature changes (results not shown). Furthermore, the length of this plateau diminishes as the proportion of the EN in the mixed film increases at any temperature studied. The $C_S^{-1}-\pi$ curves (Figure 2) obtained for the mixed monolayers are also quasi identical as compared to those for GA. These results demonstrate that the addition of the ester to GA monolayers does not provoke any condensation effect on the peptide film. In summary, one may conclude that the presence of GA causes a pronounced expansion at the interface and the behavior of the mixed monolayers is controlled by the presence of the peptide in the film. However, the fact that the transition P_1 (which can be clearly be distinguished in the compression modulus curve of EN) does not appear in the $C_S^{-1}-\pi$ dependencies for mixtures may suggest that GA and EN are miscible and interact. In addition, for GA molar ratios ≤ 0.5, the transition P_2 becomes visible as the temperature increases and follows the same trend as the collapse pressure, that is, occurs at higher surface pressures as compared to pure film.

The presence of $CaCl_2$ in the subphase (isotherms not shown) does not affect the shape of the isotherms of GA, EN, and their mixtures. However, the transition P_2 is more pronounced in the presence of divalent cations, and the collapse of the film is, in general, higher for mixtures spread on Ca^{2+}-containing subphase (Figure 3). It has been reported[26] that the presence of Na^+ shifts the isotherms of EN to smaller areas and this film contraction was significantly stronger than that observed in the presence of Ca^{2+}. This has been attributed to the interactions between EN and the subphase ions leading to their complexation at the interface.[26] As a result, the behavior of mixed monolayer changes due to the rearrangement of EN molecules at the interface, and, finally, the presence of Ca^{2+} seems to favor the miscibility of the ester and GA at the interface.

Mean Molecular Areas of GA−EN Langmuir Monolayers. To analyze the miscibility of GA and EN in the investigated mixed system, we have examined the mean area per molecule (A_{12}) as a function of the film composition (X_{GA}) at different surface pressures. A_{12} is defined as $X_1A_1 + X_2A_2$, where A_i is the mean molecular area per molecule of pure component i (1 or 2) at the particular surface pressure and X_i denotes the mole fraction of component i in the mixed monolayer. Figures 3 (NaCl-containing subphase) and 4 ($CaCl_2$-containing subphase) present the plots $A_{12}-X_{GA}$ at several surface pressures, corresponding to the expanded state, expanded-condensed transition region, and condensed state of the isotherms recorded at different temperatures. These relationships presented in solid lines and symbols are compared to the theoretical values (dashed lines) calculated following the additivity rule (obeyed for either immiscible or ideal mixtures). As it can be seen in Figure 3, at surface pressures below the transition P_3 (which occurs at 18 mN m^{-1}), the values of the mean molecular areas (A_{12}) are nearly additive at both 20 and 25 °C. However, at surface pressures above the P_3 transition, corresponding to the reorientation of GA at the interface (see values at $\pi = 25$ mN m^{-1}), the system is no longer ideal and presents negative deviations from linearity. Another observation is that these deviations diminish upon increasing subphase temperature. Thus, at the lowest temperature studied, that is, 15 °C, all of the mixtures exhibit negative deviations at any surface pressure studied. Similar results are shown in Figure 4 for monolayers spread on $CaCl_2$ aqueous subphases. However, as compared to NaCl-containing subphase, the negative deviations on $CaCl_2$ are smaller. Therefore, one may conclude that both the presence of monovalent cations and the decrease of temperature provoke a contraction of the studied mixtures at the interface.

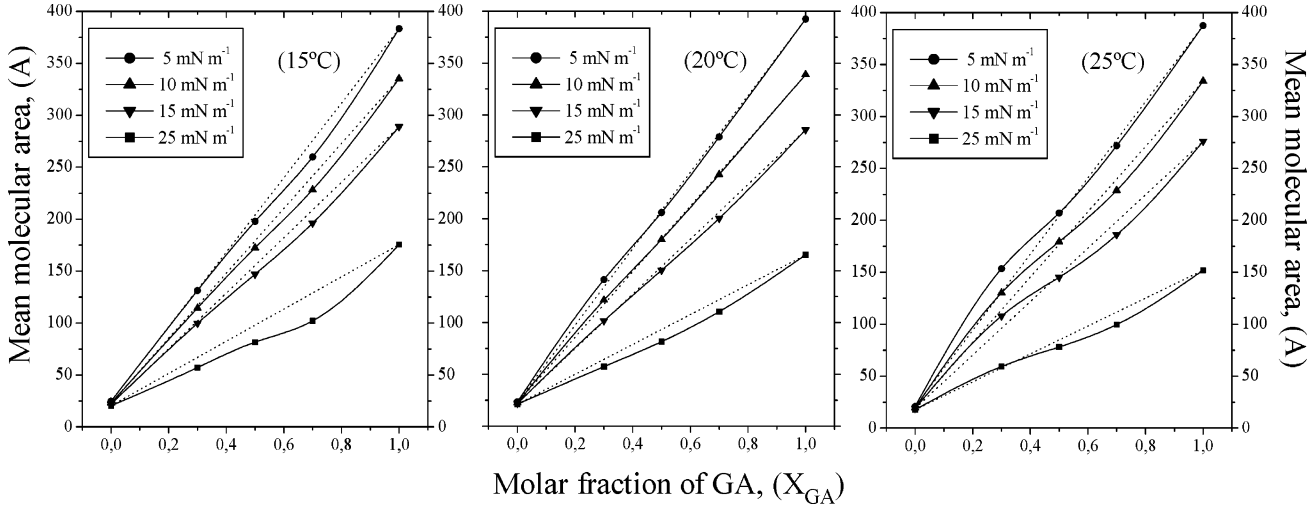

Figure 4. Plots of the mean molecular area (A) versus mole fraction of GA (X_{GA}) at different surface pressures and temperatures. Subphase: $CaCl_2$ aq, $I = 0.01$ M.

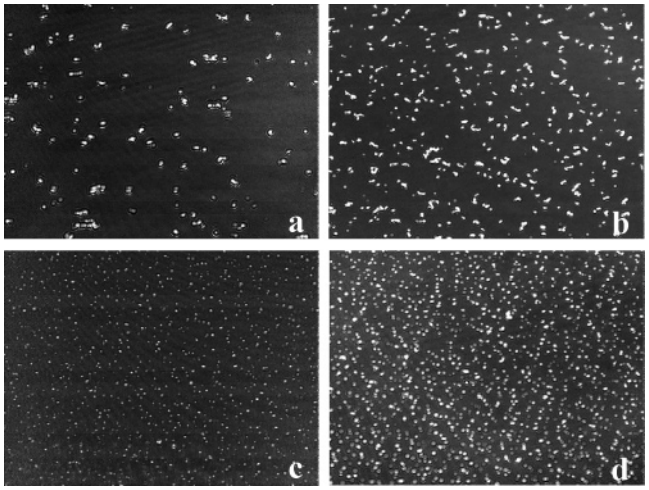

Figure 5. BAM images of mixed monolayers at 20 °C, $X_{GA} = 0.7$. Images a and b were obtained on NaCl aqueous subphases: (a) start of the expanded phase; (b) collapse. Images c and d were obtained on $CaCl_2$ aqueous subphases: (c) start of the expanded phase; (d) collapse.

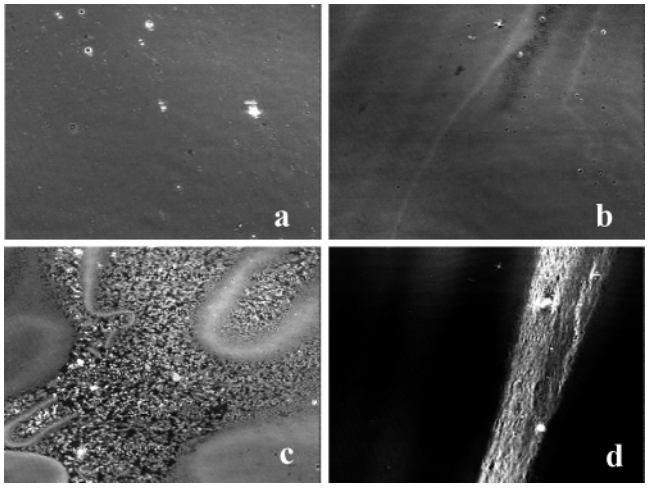

Figure 6. BAM images of mixed monolayers at 20 °C, $X_{GA} = 0.9$. Subphase: NaCl aq. (a) Liquid expanded phase; (b), (c), and (d) correspond to distinct zones of the collapsed film.

In general, the existence of deviations from linearity is attributed to the miscibility of both components interacting with each other at the interface.[32] Therefore, the negative deviations shown in Figures 3 and 4 suggest that GA and EN mix and interact in the monolayer. However, previous studies on GA and EN spread in monolayers in the absence of cations showed positive deviations at $\pi < \pi_t$ and an ideal behavior when GA is oriented vertically with respect to the interface.[34] With this in mind and assuming that both molecules are miscible at the interface, it is difficult to explain why the mixed monolayers occupy smaller areas in the presence of ions with respect to pure films. Therefore, we postpone this discussion until the morphology of the mixed monolayers is analyzed.

Morphological Studies (Brewster Angle Microscopy, BAM). To obtain a deeper insight into the behavior of the investigated mixtures, we have applied BAM for a direct observation of the monolayers structure. In this paper, we present only BAM images corresponding to the mixtures. The morphologies of pure monolayers were already presented in our previous studies.[26,33]

Figure 5a−d shows BAM images taken for mixed monolayers of $X_{GA} = 0.7$ at 20 °C. We began our studies with this molar ratio because the strongest negative deviations from the ideal behavior (see Figures 3 and 4) were observed for this particular film composition. Images a and b correspond to NaCl subphases; the first one was taken at the beginning of the expanded region, while the other one was taken at the film collapse. Both images are similar and exhibit highly dense, widespread structures, which increase in number as the surface pressure rises, and are originated due to the aggregation of molecules at the interface. Images c and d (recorded in the presence of Ca^{2+} ions) reveal only a reduction of these domain sizes with respect to those described above.

The morphology of the mixed monolayers significantly differs from those obtained for pure films.[26,33] EN forms dense and large bright structures only at the collapse,[26] and GA monolayers exhibit small bright nuclei only in the presence of Ca^{2+} at surface pressures above 18 mN m^{-1} and at low temperature (15 °C).[33] Thus, it is obvious that in the binary system, one component starts to aggregate in the presence of the other, and this process occurs at surface pressures above 3−4 mN m^{-1}. Taking into account that only GA forms similar bright nuclei at low temperatures, it seems that the aggregation of GA molecules at $\pi < \pi_c$ is the most logical explanation for the nuclei formation in mixed monolayer.

Results shown in Figure 6a−d ($X_{GA} = 0.9$) demonstrate that upon increasing the proportion of the peptide, the number of nuclei in the monolayer decreases (image a) (similar results were

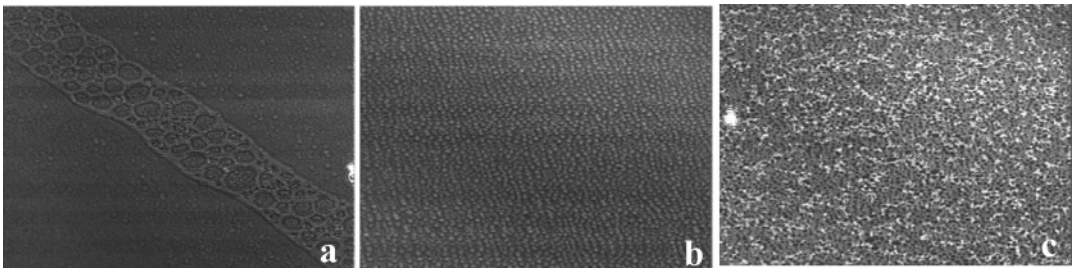

Figure 7. BAM images of mixed monolayers at 20 °C, $X_{GA} = 0.1$. Subphase: NaCl aq. (a) Transition from gas to liquid expanded phase; (b) transition from liquid expanded to liquid condensed phase; (c) collapse.

obtained in the presence of Ca^{2+}). Thus, supposing that these aggregates are formed by GA molecules, they should increase in number or size as the proportion of GA increases. However, Figure 6a shows a homogeneous film (which resembles pure monolayer of GA) with a very low number of dispersed nuclei. Thus, changes observed in the film morphology upon increasing the molar ratio of GA are consistent with the ester molecules forming three-dimensional nuclei in the mixed monolayer.

Images b, c, and d in Figure 6 correspond to distinct regions of the collapsed monolayer. Image b exhibits the characteristic morphology of pure GA monolayer with characteristic fractures lines. Image d shows how the molecular aggregation of EN is more effective along these fractures and dense, large three-dimensional structures can be distinguished. These zones coexist with regions of different appearance (image c of Figure 6), which exhibit morphology similar to that observed during the collapse of a mixed monolayer where $X_{GA} < 0.3$ (Figure 7). For this particular monolayer composition (where the proportion of peptide is low), the obtained images are typical of a gas phase (image a) and of a liquid expanded−liquid condensed transition (image b). These morphologies were not observed for mixed monolayers in which $X_{GA} \geq 0.3$ (results not shown and similar to those seen for $X_{GA} = 0.7$ in Figure 5), where the bright nuclei started to appear in the region of low values of π (3−4 mN m^{-1}) until the end of compression. Furthermore, Figure 7c shows that ester molecules are not expelled from the monolayer to form solid aggregates even during the collapse of the film. Images taken for monolayers spread in the presence of Ca^{2+} (results not shown) showed morphologies and behavior similar to those described above in the presence of Na^+. Only a slight decrease in the efficiency of molecular aggregation of EN was observed due to the presence of divalent cations. This effect has already been noted in pure monolayers of EN and was significantly more pronounced in absence of ions.[26]

In the former paragraph, we postponed the discussion concerning the miscibility of both components in the binary system until BAM analysis is done. At this point, we can ensure that negative deviations displayed in the $A_{12}-X_{GA}$ plots cannot be simply ascribed as being due to both components being miscible and interacting at the interface. On the contrary, the observed contraction is a consequence of squeezing out the ester molecules from the mixed monolayer and subsequent formation of solid three-dimensional nuclei at very low surface pressures. It is thus evident that GA and EN are immiscible at the interface at $X_{GA} \geq 0.3$ and EN molecules are squeezed out from the monolayer. Thus, upon increasing molar ratios of GA above 0.3, the following three phases coexist at the interface: the solid three-dimensional nuclei of EN, regions covered with GA molecules, and small zones of mixed monolayer at $X_{GA} < 0.3$.

Conclusions

Mixed monolayers composed of EN and GA were spread on aqueous subphases containing Na^+ and Ca^{2+}. Their behavior was studied at three different temperatures (15, 20, and 25 °C) using surface pressure−area (π/A) isotherms complemented with BAM images. The obtained results allowed us to conclude the following:

(1) The presence of GA in mixtures with EN causes a pronounced expansion at the interface, and the behavior of mixed monolayers is controlled by the presence of GA in the film.

(2) Compression moduli versus surface pressure plots demonstrate that GA and EN mix at surface pressures below 5 mN m^{-1} for any experimental condition studied. At higher surface pressures, the miscibility depends on the molar ratio and increases in the presence of Ca^{2+} and upon increasing the temperature.

(3) The mean molecular area values indicate that the additivity rule is obeyed for mixtures at surface pressures below the phase transition characteristic for GA, while at higher π the negative deviations are observed. The strength of these deviations increases in the presence of monovalent cations and the decrease of subphase temperature.

(4) Based solely on the analysis of π/A isotherms, the negative deviations observed in the $A_{12}-X_{GA}$ plots can be interpreted as being due to interacting molecules in a miscible, mixed monolayer. However, the application of the microscopic surface-sensitive technique (BAM) allowed for a better understanding of the investigated system. Mixed monolayer morphology revealed that for mixtures of low GA content (below GA mole fraction of 0.3), both components are miscible, while at $X_{GA} \geq 0.3$, GA and EN do not mix.

(5) BAM images proved that the observed contraction of mean molecular areas is a consequence of squeezing out ester molecules from the mixed monolayer to form solid nuclei. The efficiency of this process, which only occurs when cations are dissolved in the subphase, increases at low temperatures and in the presence of Na^+.

(6) Taking into consideration the results presented in the present work, the optimum artificial membrane refers to a mixed GA−EN film of $X_{GA} < 0.3$, which can be transferred onto solid supports at surface pressures above 18−20 mN m^{-1}, allowing the vertical orientation of GA molecules in the mixed monolayer.

Acknowledgment. This work was supported by Ministerio de Ciencia y Tecnología (grant BQU2003-00949) and Xunta de Galicia (grant PGIDT04PXIC38303PN).

References and Notes

(1) Wallace, B. A. *J. Struct. Biol.* **1998**, *121*, 123−141.
(2) Sarges, R.; Witkop, B. *J. Am. Chem. Soc.* **1965**, *87*, 2011−2020.

(3) Arseniev, A. S.; Barsukov, I. L.; Bystrov, V. F.; Lomize, A. L.; Ovchinnikov, Y. A. *FEBS Lett.* **1985**, *186*, 168−174.
(4) Ketchem, R. R.; Roux, B.; Cross, T. A. *Science* **1993**, *261*, 1457−1460.
(5) Arseniev, A. S.; Barsukov, I. L.; Bystrov, V. F. *FEBS Lett.* **1985**, *180*, 33−39.
(6) Burkhart, B. M.; Lee, N.; Langs, D. A.; Pangborn, W. A.; Duax, W. L. *Proc. Natl. Acad. Sci. U.S.A.* **1998**, *95*, 12950−12955.
(7) Killian, J. A.; Urry, D. W. *Biochemistry* **1988**, *27*, 7295−7301.
(8) Cox, K. J.; Ho, C.; Lombardi, J. V.; Stubbs, C. D. *Biochemistry* **1992**, *31*, 1112−1117.
(9) Franks, N. P.; Lieb, W. R. *Nature* **1982**, *300*, 487−493.
(10) Franks, N. P.; Lieb, W. R. *Nature* **1986**, *319*, 77−78.
(11) Franks, N. P.; Lieb, W. R. *Nature* **1988**, *333*, 662−664.
(12) Hendry, B. M.; Elliott, J. R.; Haydon, D. A. *Proc. R. Soc. London, Ser. B: Biol. Sci.* **1985**, *224*, 389−397.
(13) Haydon, D. A.; Henry, B. M.; Lewinson, S. R.; Requena, J. *Nature* **1977**, *268*, 356−358.
(14) Haydon, D. A. *Ann. N.Y. Acad. Sci.* **1975**, *264*, 2−16.
(15) Hladky, S. B.; Haydon, D. A. *Curr. Top. Membr. Transp.* **1984**, *21*, 327−372.
(16) Salom, D.; Abad, C.; Braco, L. *Biochemistry* **1992**, *31*, 8072−8079.
(17) Scarlata, S. F. *Biochemistry* **1991**, *30*, 9853−9859.
(18) Nelson, A. *Langmuir* **1997**, *13*, 5644−5651.
(19) Ducharme, D.; Vaknin, D.; Paudler, M.; Salesse, C.; Riegler, H.; Möhwald, H. *Thin Solid Films* **1996**, *284−285*, 90−93.
(20) Mobashery, N.; Nielsen, C.; Andersen, O. S. *FEBS Lett.* **1997**, *412*, 15−20.
(21) Galbraith, T. P.; Wallace, B. A. *Faraday Discuss.* **1998**, *111*, 159−164.
(22) Salom, D.; Pérez-Payá, E.; Pascal, J.; Abad, C. *Biochemistry* **1998**, *37*, 14279−12291.
(23) Doyle, D. A.; Wallace, B. A. *Biophys. J.* **1998**, *75*, 635−640.
(24) Gaines, G. L., Jr. *Insoluble Monolayers at Liquid−Gas Interface*; Interscience: New York, 1966.
(25) Nieto-Suárez, M.; Vila-Romeu, N.; Dynarowicz-Latka, P.; Prieto, I. *Colloids Surf., A* **2004**, *249*, 11−14.
(26) Nieto-Suárez, M.; Vila-Romeu, N.; Prieto, I. *Appl. Surf. Sci.* **2005**, *246*, 387−391.
(27) Hönig, D.; Möbius, D. *Thin Solid Films* **1992**, *210/211*, 64−68.
(28) Möbius, D. *Curr. Opin. Colloid Interface Sci.* **1996**, *1*, 250−256.
(29) Vila, N.; Puggelli, M.; Gabrielli, G. *Colloids Surf., A* **1996**, *119*, 95−104.
(30) Tournois, H.; Gieles, P.; Demel, R.; de Gier, J.; De Kruijff, B. *Biophys. J.* **1989**, *55*, 557−569.
(31) Davion-Van Mau, N.; Daumas, P.; Lelièvre, D.; Trudelle, Y.; Heitz, H. *Biophys. J.* **1987**, *51*, 843−845.
(32) Dynarowicz-Latka, P.; Kita, K. *Adv. Colloid Interface Sci.* **1999**, *79*, 1−17.
(33) Vila-Romeu, N.; Nieto-Suárez, M.; Dynarowicz-Latka, P.; Prieto, I. *J. Phys. Chem. B* **2002**, *106*, 9820−9824.
(34) Vila-Romeu, N.; Nieto-Suárez, M.; Castro-Silva, M. *Colloids Surf.*, accepted for publication.